RA

DRFC-CAD

EUR-CEA-FC-1347

IGNITION IN NET FOR DIFFERENT ENERGY CONFINEMENT TIME SCALINGS

J. JOHNER, F. PREVOT

June 1988

CEA EURATOM

ASSOCIATION EURATOM-C.E.A
DEPARTEMENT DE RECHERCHES SUR LA FUSION CONTROLEE
C.E.N. CADARACHE
13108 SAINT PAUL LEZ DURANCE CEDEX

DRFC-CAD EUR-CEA-FC-1347

IGNITION IN NET FOR DIFFERENT ENERGY CONFINEMENT TIME SCALINGS

J. JOHNER, F. PREVOT

June 1988

IGNITION IN NET FOR DIFFERENT ENERGY CONFINEMENT TIME SCALINGS

J. JOHNER, F. PREVOT

ASSOCIATION EURATOM-CEA SUR LA FUSION
Département de Recherches sur la Fusion Contrôlée
Centre d'Etudes Nucléaires de Cadarache
13108 SAINT-PAUL-LEZ-DURANCE CEDEX (FRANCE)

ABSTRACT

A zero-dimensional profile dependent model is used to assess the feasibility of ignition in the extended version of NET. Five recent scalings for the energy confinement time (Goldston, Kaye All, Kaye Big, Shimomura-Odajima, Rebut-Lallia) are compared in the frame of two different scenarii, i.e., H-mode with a flat density profile or L-mode with a peaked density profile. For the flat density H-mode case, ignition is accessible with none of the scalings except Rebut-Lallia's. For the peaked density L-mode case, ignition is accessible with none of the scalings exept Rebut-Lallia's. For the two Kaye's scalings, ignition is forbidden in H-mode even with the peaked density profile. For the Rebut-Lallia scaling, ignition is allowed in L-mode even with the flat density profile.

I. INTRODUCTION

Five different scalings for the global energy confinement time with strong additional heating have recently emerged [1] as potential candidates for ITER studies. The old Goldston [2] scaling has shown remarkable agreement with experimental datas. Kaye [1] has derived two new different scalings according to all machines of his data base or only the large ones (DIII-D, TFTR, JT-60, JET) are considered in the statistical analysis (they differ only by the exponents of R and a). The $I_p^{1.24}$ dependence of the old Kaye-Godston scaling [3] is now generally considered as too optimistic. Results for this up-to-now widely used scaling will only be given for reference purposes. The semi-empirical Rebut-Lallia [4] heat diffusivity leads to an offset-linear global energy confinement time scaling with shows good agreement with experimental datas as well as the Shimomura-Odajima scaling [5].

In the present paper, the zero-dimensional ignition power balance equation (P_{add}=0) including the effects of elongation, density and temperature profiles, and dilution due to alpha particles and to two light impurity species is solved for the above five scalings. This type of global model is similar to that used by Uckan et al. [6] which has been shown to give good agreement with the 1-1/2-D WHIST transport code. The analysis is performed for the enhanced plasma size version of NET DN [7] for two different scenarii, i.e.,

1/ flat density profile $n \propto (1-\rho^2)^{0.5}$ representative of the H-mode,

2/ peaked density profile $n \propto (1-\rho^2)^2$ which is thought to be an alternative approach to ignition in the L-mode.

MKSA units are used throughout the paper except for the temperature which is always expressed in keV ($k=1.6022\times10^{-16}$ J/keV).

II. THE MODEL

1. The geometry

The magnetic surfaces are supposed to be a set of concentric and similar ellipses of equation

$$\frac{x^2}{a^2} + \frac{y^2}{\kappa^2 a^2} = \rho^2$$

where κ=b/a is the poloidal section elongation and ρ is the radial elliptical coordinate. In the large aspect ratio limit, the relation between the safety factor q_{cyl} at the plasma surface and the total current is

$$I_p = \frac{2\pi}{\mu_o}\,\frac{1+\kappa^2}{2}\,\frac{B_t a}{A q_{cyl}}$$

where A=R/a is the torus aspect ratio. The plasma shape triangularity is not considered in the present paper. The relation between the MHD safety factor q_ψ at the edge and q_{cyl} is taken to be [8]

$$q_\psi = q_{cyl}\,\frac{1.22-0.68/A}{(1-1/A^2)^2}$$

2. The thermal equilibrium equation

The following steady state power balance equation is solved numerically

$$P_\alpha(\langle n\rangle,[T]) + P_\Omega([T]) + P_{add} = P_B(\langle n\rangle,[T]) + \frac{W_{th}(\langle n\rangle,[T])}{\tau_E(\langle n\rangle,P_{tot})}$$

with

$$P_{tot} = P_\alpha + P_\Omega + P_{add}$$

where $\langle n\rangle$ is the volume averaged electron density and [T] the density averaged plasma temperature (we assume $T_e=T_i=T$). P_α is the alpha power source including the effect of dilution due to alpha particles and to two light impurity species

$$P_\alpha(\langle n\rangle,[T]) = C_{Z\alpha}\,\frac{\langle n\rangle^2}{4}\,\overline{\sigma v}^*([T])\,F_\alpha E_\alpha\,V$$

where F_α is the fraction of the alpha particle power source which is deposited into the plasma (we take $F_\alpha=1$) and

$$C_{Z\alpha} = \left[\frac{Z_1(Z_1-Z_{eff})+r_{21}Z_2(Z_2-Z_{eff}) - 2f_\alpha[Z_1(Z_1-2)+r_{21}Z_2(Z_2-2)]}{Z_1(Z_1-1)+r_{21}Z_2(Z_2-1)}\right]^2$$

where Z_{eff} is the plasma effective charge which is supposed to have a flat profile, Z_1 and Z_2 are the charges of the two impurity ions, $r_{21}=n_2/n_1$ is the ratio between the two impurity densities, $f_\alpha=n_\alpha/n$ is the equilibrium alpha particle fraction and $V=2\pi^2 A\kappa a^3$ is the plasma volume. Following the US-ITER recommendation [9], we suppose $Z_{eff}=1.8$, $f_\alpha=5\%$, and an equal mixture of C(6) and O(8) [$Z_1=6$, $Z_2=8$, $r_{21}=1$]. In these conditions, we obtain $C_{Z\alpha} \simeq 0.618$. $\overline{\sigma v}^*$ is the effective thermonuclear reaction rate taking into account the density and temperature profiles. Choosing the following profiles

$$n = n_o(1-\rho^2)^{\alpha_n} \quad \text{and} \quad T = T_o(1-\rho^2)^{\alpha_T} \qquad (1)$$

giving

$$\frac{n_e}{\langle n\rangle} = 1+\alpha_n \qquad \text{and} \qquad \frac{T_e}{[T]} = \frac{1+\alpha_n+\alpha_T}{1+\alpha_n}$$

we obtain

$$\overline{\sigma v}^*(\alpha_n,\alpha_T,[T]) = (1+\alpha_n)^2 \int_0^1 u^{2\alpha_n}\, \overline{\sigma v}\left[\frac{1+\alpha_n+\alpha_T}{1+\alpha_n}\, u^{\alpha_T}[T]\right] du$$

The above function is calculated numerically using the Peres [10] fit for $\overline{\sigma v}(T)$. P_Ω is the ohmic power calculated using a simplified Spitzer resistivity

$$\eta = Z_{eff}\,\frac{\eta_o}{T^{3/2}} \quad \text{with} \quad \eta_o = 3\times10^{-8}$$

The radial integration can be performed exactly in this case, we obtain

$$P_\Omega([T]) = Z_{eff}\,\eta_o^*\left[\frac{I_p}{S_p}\right]^2 \frac{1}{[T]^{3/2}}\,V \quad \text{where} \quad S_p = \pi\kappa a^2$$

with

$$\eta_o^* = \frac{(1+\alpha_n)^{3/2}(1+3\alpha_T/2)}{(1+\alpha_n+\alpha_T)^{3/2}}\,\eta_o$$

P_B is the bremsstrahlun radiation loss calculated using the non-relativistic Born approximation

$$P_B(\langle n\rangle,[T]) = Z_{eff}\,C_B^*\,\langle n\rangle^2\,[T]^{1/2}\,V$$

with

$$C_B^* = \frac{(1+\alpha_n)^{3/2}(1+\alpha_n+\alpha_T)^{1/2}}{1+2\alpha_n+\alpha_T/2}\,C_B$$

and

$$C_B = \frac{1}{(4\pi\varepsilon_o)^3}\,\frac{32\sqrt{2}}{3\sqrt{\pi}}\,\frac{e^6 k^{1/2}}{m_e^{3/2}c^3\hbar} \simeq 5.355\times10^{-37}$$

W_{th} is the total plasma thermal content (not including the fast alpha contribution)

$$W_{th} = C_{ZW}\,3\langle n\rangle k[T]\,V$$

with

$$C_{ZW} = 1 - \frac{(Z_{eff}-1)[Z_1-1+r_{21}(Z_2-1)] + f_\alpha[(Z_1-1)(Z_1-2)+r_{21}(Z_2-1)(Z_2-2)]}{2[Z_1(Z_1-1)+r_{21}Z_2(Z_2-1)]} \quad (2)$$

with the above values for Z_{eff}, f_α, Z_1, Z_2 and r_{21}, we obtain $C_{ZW} \simeq 0.926$.

3. The confinement time scalings

In the present paper, we consider five different scalings for the energy confinement time which have been shown to give equally good behaviour when compared to the L-mode experimental datas. They are the scalings proposed by Goldston [2], Kaye (All and Big) [1], Shimomura-Odajima [5] and Rebut-Lallia [4].

a/ The L-mode scalings

We have the following explicit expression in MKSA units

1/ Goldston scaling (ohmic heating negligible)

$$\tau_{EG} = C_{\tau G} \frac{M_{eff}^{1/2}\, \kappa^{1/2}\, I_p\, R^{1.75}}{a^{0.37}\, P_{tot}^{1/2}}$$

with

$$C_{\tau G} = \frac{6.4\times10^{-5.24}}{(1.5)^{1/2}} \simeq 3.01\times10^{-5}$$

2/ Kaye All scaling (All machines of the data base, ohmic heating negligible)

$$\tau_{EKA} = C^*_{\tau KA} \frac{M_{eff}^{1/2}\, \kappa^{1/4}\, I_p^{0.85}\, \langle n\rangle^{0.1}\, B_t^{0.3}\, R^{0.85}\, a^{0.3}}{P_{tot}^{1/2}}$$

with

$$C^*_{\tau KA} = (\bar{n}/\langle n\rangle)^{0.1}\, C_{\tau KA} \quad \text{and} \quad C_{\tau KA} = 5.21\times10^{-6}$$

where $\bar{n}/\langle n\rangle$ is the ratio of the line averaged to the volume averaged density. With the profile given in Eq.(1), we obtain

$$\frac{\bar{n}}{\langle n\rangle} = (1+\alpha_n)\, 2^{2\alpha_n} \frac{\Gamma^2(1+\alpha_n)}{\Gamma(2+2\alpha_n)}$$

where Γ is the Euler gamma function.

3/ Kaye Big scaling (Big machines of the data base: DIII-D, TFTR, JT-60, JET, ohmic heating negligible)

$$\tau_{EKB} = C^{*}_{\tau KB} \frac{M_{eff}^{1/2}\,\kappa^{1/4}\,I_p^{0.85}\,\langle n\rangle^{0.1}\,B_t^{0.3}\,R^{0.5}\,a^{0.8}}{P_{tot}^{1/2}}$$

with

$$C^{*}_{\tau KB} = (\bar{n}/\langle n\rangle)^{0.1}\,C_{\tau KB} \quad \text{and} \quad C_{\tau KB} = 8.2\times10^{-6}$$

4/ Shimomura-Odajima scaling (including the ohmic case)

$$\tau_{ESO} = C^{(1)*}_{\tau SO} \frac{M_{eff}^{1/2}\,\kappa^{0.2}\,I_p\,\langle n\rangle^{0.6}\,B_t^{0.2}\,R^{1.6}\,a^{0.4}\,f(Z_{eff})g(q_{cyl})}{P_{tot}} + \ldots$$

$$+ C^{(2)}_{\tau SO}\,M_{eff}^{1/2}\,\kappa a^{2}$$

with

$$C^{(1)*}_{\tau SO} = (\bar{n}/\langle n\rangle)^{0.6}\,C^{(1)}_{\tau SO} \quad \text{and} \quad C^{(1)}_{\tau SO} = 1.56\times10^{-13.4} \simeq 6.21\times10^{-14}$$

$$C^{(2)}_{\tau SO} = 8.49\times10^{-2}$$

$$f(Z_{eff}) = Z_{eff}^{0.4}\left[\frac{15-Z_{eff}}{20}\right]^{0.6}, \quad g(q_{cyl}) = \left[\frac{3q_{cyl}(q_{cyl}+5)}{(q_{cyl}+2)(q_{cyl}+7)}\right]^{0.6}$$

5/ Rebut-Lallia scaling (including the ohmic case)

$$\tau_{ERL} = C^{(1)*}_{\tau RL} \frac{M_{eff}^{1/2}\,Z_{eff}^{1/4}\,I_p^{1/2}\,\langle n\rangle^{3/4}\,B_t^{1/2}\,(R\kappa a^{2})^{11/12}}{P_{tot}} + \ldots$$

$$+ C^{(2)}_{\tau RL} \frac{M_{eff}^{1/2}}{Z_{eff}^{1/2}}\,I_p(R\kappa a^{2})^{1/2}$$

with

$$C^{(1)*}_{\tau RL} = (\bar{n}/\langle n\rangle)^{3/4}\,C^{(1)}_{\tau RL} \quad \text{and} \quad C^{(1)}_{\tau RL} = 3.68\times10^{-13.25} \simeq 2.07\times10^{-13}$$

$$C^{(2)}_{\tau RL} = 1.70\times10^{-8}$$

• For the Kaye-Goldston scaling (ohmic heating negligible), we take

$$\tau_{EKG} = C^{*}_{\tau KG} \frac{M_{eff}^{1/2}\,\kappa^{0.28}\,I_p^{1.24}\,\langle n\rangle^{0.26}\,R^{1.65}}{B_t^{0.09}\,a^{0.49}\,P_{tot}^{0.58}}$$

with

$$C^{*}_{\tau KG} = (\bar{n}/\langle n\rangle)^{0.26}\,C_{\tau KG} \quad \text{and} \quad C_{\tau KG} = \frac{2.77\times10^{-10.86}}{(1.5)^{1/2}} \simeq 3.12\times10^{-11}$$

• Remarks on the numerical coefficients and M_{eff} dependences

- The original Goldston scaling [2] is supposed to be valid for M_{eff}=1.5. An additional $(M_{eff}/1.5)^{1/2}$ dependence is added. This is consistent with the expression of Ref. [1].

- For the two Kaye scalings, the expression of Ref. [1] is taken.

- For the Rebut-Lallia scaling, the expression of Ref. [1] is taken. It is consistent with the original expression of Ref. [4] (supposed to be valid for M_{eff}=2) if the total energy confinement time is assumed to be twice the electron energy confinement time. An additional $(M_{eff}/2)^{1/2}$ dependence has been added.

- For the Shimomura-Odajima scaling, the expression of Ref. [1] is retained.

- The original Kaye-Goldston scaling [3] is supposed to be valid for M_{eff}=1.5. An additional $(M_{eff}/1.5)^{1/2}$ dependence is added. This is consistent with the expression of Ref. [1].

b/ <u>The global energy confinement time for L and H modes</u>

1/ In the case of the monomial scalings (Goldston, Kaye All, Kaye Big, Kaye-Goldston), the global energy confinement time is taken following the Goldston prescription [2]

$$\tau_E = \left[1/\tau_{NA}^2 + 1/(f_L \tau_{Ex})^2\right]^{-1/2}$$

where τ_{ENA} is the neo-Alcator scaling

$$\tau_E = C^*_{\tau NA} \langle n \rangle R^2 a\, q_{cyl}$$

with

$$C^*_{\tau NA} = (\bar{n}/\langle n \rangle)\, C_{\tau NA} \quad \text{and} \quad C_{\tau NA} = 7\times10^{-22}$$

Note that no κ and M_{eff} dependence are retained in the neo-Alcator scaling.

f_L is the enhancement factor of the confinement time in H-mode relative to the L-mode. The value of f_L which fits the experimental datas is different for each scaling. Following the Kaye [1] prescription (including the JFT2M points), we take the following values

Goldston : $f_L = 1.9$

Kaye All : $f_L = 2.4$

Kaye Big : $f_L = 2.1$

Kaye-Goldston : $f_L = 2.2$

2/ In the case of the offset-linear scalings (Shimomura-Odajima, Rebut-Lallia) the global confinement time is simply

$$\tau_E = f_L \tau_{Ex}$$

Now, we take [1]

Shimomura-Odajima : $f_L = 1.4$

Rebut-Lallia : $f_L = 1.6$

4. The operating window

a/ Beta limit

We suppose that operation is restricted to the first MHD stability regime with the usual Troyon limit on beta, i.e., $\langle\beta\rangle < \langle\beta\rangle_T$ with

$$\langle\beta\rangle = C_{ZW} \frac{2\langle n\rangle k[T]}{B_t^2/2\mu_o}$$

with C_{ZW} given in Eq.(2) and

$$\langle\beta\rangle_T = 10^{-8}\, g \frac{I_p}{B_t a}$$

where g is the Troyon parameter. We take g=3. It is important to remark that the fast alpha contribution to beta is not considered in the present work.

b/ Density limit

The Murakami density limit is also calculated

$$\langle n\rangle_M = C_M^* \frac{B_t}{Rq_{cyl}} \quad \text{with} \quad C_M^* = \frac{C_M}{\bar{n}/\langle n\rangle} \quad \text{and} \quad 1.5\times10^{20} < C_M < 3\times10^{20}$$

Murakami (2) [or $\langle n\rangle_M^{(2)}$] and Murakami (3) [or $\langle n\rangle_M^{(3)}$] will refer to $C_M = 2\times10^{20}$ and $C_M = 3\times10^{20}$ respectively.

III. MACHINE PARAMETERS AND RESULTS

1. Machine parameters and profiles

The parameters of NET [7] are given in Table I. We only consider the enhanced plasma size DN version. We take M_{eff}=2.5. We also recall that we have supposed Z_{eff}=1.8 with Z_1=6, Z_2=8, r_{21}=1 and f_α=5%.

The temperature profile is supposed to be parabolic (α_T=1). Different values of the density peaking parameter α_n are considered in the following. The density profile

$$\frac{n(\rho)}{<n>} = (1+\alpha_n)\ (1-\rho^2)^{\alpha_n}$$

is represented in Fig.1 for α_n=0.5, 1, 2.

2. Results for a flat density profile (α_n=0.5)

Ohmic ignition curves (P_{add}=0) in the (<n>,[T]) plane are represented for the different scalings and different values of the L-mode enhancement factor f_L. The Troyon beta limit (g=3) and Murakami (2) and (3) density limits are also represented.

• For the Goldston scaling (Fig.2), ignition curves are drawn for f_L=2.5, 2.127, 2.11, 2.102. For the Kaye prescription for the H-mode, f_L=1.9, the high temperature branch of the ohmic ignition curve does not exist, it vanishes for f_L=2.1017251 as illustrated in Fig.3.

• For the Kaye All scaling (Fig.4), ignition curves are drawn for f_L=4, 3.415, 3.2, 3.1. For the Kaye prescription for the H-mode, f_L=2.4, the ignition curve is not accessible.

• For the Kaye Big scaling (Fig.5), ignition curves are drawn for f_L=3.5, 3.022, 2.8 and 2.7. For the Kaye prescription for the H-mode, f_L=2.1, the ignition curve is not accessible.

• For the Shimomura-Odajima scaling (Fig.6), ignition curves are drawn for f_L=2.5, 1.927, 1.4, and 1. For the Kaye prescription for the H-mode, f_L=1.4, the ignition curve is not accessible.

• For the Rebut-Lallia scaling (Fig.7), ignition curves are drawn for f_L=1.6, 1.4, 1.2, and 1. Ignition is accessible even in the L-mode (f_L=1). The Kaye prescription is f_L=1.6.

- For the Kaye-Goldston scaling (Fig.8), ignition curves are drawn for f_L=2.2, 1.765, 1.7, 1.6. For the Kaye prescription for the H-mode, f_L=2.2, the ignition curve is accessible.

3. Results for a peaked density profile (α_n=2)

- For the Goldston scaling (Fig.9), ignition curves are drawn for f_L=1.9, 1.75, 1.686, 1.6815. For L-mode operation, the high temperature branch of the ohmic ignition curve does not exist, it vanishes for f_L=1.6814. In H-mode with f_L=1.9 (Kaye), ignition would be accessible with such a profile.

- For the Kaye All scaling (Fig.10), ignition curves are drawn for f_L=3, 2.655, 2.5, 2.4. Even in H-mode with f_L=2.4 (Kaye), the ignition curve is not accessible.

- For the Kaye Big scaling (Fig.11), ignition curves are drawn for f_L=3, 2.350, 2.2, 2.1. Even in H-mode with f_L=2.1 (Kaye), the ignition curve is not accessible.

- For the Shimomura-Odajima scaling (Fig.12), ignition curves are drawn for f_L=2, 1.4, 1.326 and 1. In H-mode with f_L=1.4, ignition would be accessible with such a profile.

- For the Rebut-Lallia scaling (Fig.13), ignition curves are drawn for f_L=1.6, 1.4, 1.2, and 1. Ignition is accessible in L-mode (f_L=1).

- For the Kaye-Goldston scaling (Fig.14), ignition curves are drawn for f_L=1.5, 1.375, 1.3, 1.24. Ignition is not accessible in L-mode with this scaling.

4. Results for a varying density profile

In Fig.15, the critical f_L value required for contact between the high temperature branch of the ignition curve and the Troyon beta limit curve is represented in terms of α_n for the different scalings. This figure shows the hierarchy of the scalings when applied to NET. The most conservative is Kaye All, then Kaye Big, Goldston, Shimomura-Odajima, the most favourable beeing Rebut-Lallia.

IV. CONCLUSION

POPCON analysis of ignition in NET DN with enhance size and five different scalings for τ_E gives relatively pessimistic results. The criterion which is considered for the feasibility of ignition is the existence of part of the high temperature branch of the ignition curve below the Troyon beta limit curve with g=3.

- For the Kaye All scaling, the L-mode enhancement factor f_L required for ignition is 3.415 for α_n=0.5 and 2.655 for α_n=2. Both values are above the prescribed value f_L=2.4.

- For the Kaye Big scaling, the L-mode enhancement factor f_L required for ignition is 3.022 for α_n=0.5 and 2.350 for α_n=2. Both values are above the prescribed value f_L=2.1.

- For the Goldston scaling, f_L=2.127 is required for α_n=0.5 and 1.686 for α_n=2. The prescribed value of f_L beeing 1.9, ignition would be accessible in this case in NET if a peaked density profile could be sustained in H-mode.

- For the Shimomura-Odajima scaling, f_L=1.927 is needed for ignition in the case α_n=0.5 and 1.326 for α_n=2. The prescribed value of f_L beeing 1.4, we have the same conclusion as for the Goldston scaling.

- The Rebut-Lallia scaling is much more favourable than the other laws. With this scaling, ignition is possible in NET in L-mode even in the flat density case.

The contribution of the fast alpha particles to the beta and to the energy content is neglected in the present analysis. This contribution is of the order of 5-10% in the 10-15 keV range of interest here [6]. The inclusion of this effect would worsen the conclusion.

On the other hand, ignition is characterised by a power input profile which is more peaked than that of the external additional power dominated discharges used to derive present energy confinement time scalings. It has been pointed out that this could result in an improvement of the global energy confinement time. To quantify this effect, a 1-D analysis using local transport coefficients should be used.

From the present paper, it appears clearly that extensive study of the energy confinement time scaling in large machines (especially in H-mode) is required in order to come to a consensus for the ITER parameters (if ignition is desired in such a device).

REFERENCES

[1] KAYE, S.M., *Survey of Energy Confinement Scaling Expressions*, ITER Specialists' Meeting on Confinement, Garching, FRG (May 24-27, 1988).

[2] GOLDSTON, R., Plasma Physics and Controlled Fusion **26** (1984) 87.

[3] KAYE, S.M., GOLDSTON, R.J., Nucl. Fusion **25** (1985) 65.

[4] LALLIA, P.P., REBUT, P.H., WATKINS, M.L., *Chaotic Magnetic Topology and Heat Transport in Tokamaks*, JET-P(88)05 (January 1988); also Ref. [1].

[5] SHIMOMURA, Y., ODAJIMA K., JAERI Report 88-068 (March 1988); also Ref. [1].

[6] UCKAN, N.A., TOLLIVER, J.S., HOULBERG, W.A., ATTENBERGER, S.E., ORNL/TM-10612 (November 1987) presented at the Workshop on Alpha Particles Effects in ETR, Germantown, Maryland, June 15-16 (1987), Proceedings to be published in *Fusion Technology*.

[7] ENGELMANN, F., NET Report EUR-FU/XII-80/86/64 (October 1986).

[8] UCKAN, N.A., SHEFFIELD, J., in *Tokamak Start-up*, edited by H. Knoepfel, Plenum Press, New York (1986) 45.

[9] UCKAN, N.A., ITER Specialists' Meeting on Confinement, Garching, FRG (May 24-27, 1988).

[10] PERES, A., J. Appl. Phys. 50 (1979) 5569.

TABLES

TABLE I. NET ON ENHANCED SIZE PARAMETERS [(*) CALCULATED]

Machine	NET
a(m)	1.68
κ	2.17
R(m)	5.41
B_t(T)	4.8
I_p(MA)	14.8
D(m)(*)	3.65
A(*)	3.22
V(m^3)(*)	654
q_{cyl}(*)	2.41
q_ψ(*)	2.98
$\langle\beta\rangle_T$(%)(*)	5.51
$\langle n\rangle_M^{(*)}$($10^{19} m^{-3}$)(*)	6.24
$\langle n\rangle_M^{(*)}$($10^{19} m^{-2}$)(*)	9.36

FIGURES CAPTIONS

FIG. 1. Density profile $n/\langle n\rangle$ for α_n=0.5, 1, 2.

FIG. 2. NET, α_n=0.5, Goldston scaling. Ohmic ignition curves for f_L=2.5, 2.127, 2.11, 2.102. Murakami and beta limits.

FIG. 3. NET, α_n=0.5, Goldston scaling. High temperature branch of the ohmic ignition curve, f_L=2.10177, 2.10175, 2.10173, 2.1017252.

FIG. 4. NET, α_n=0.5, Kaye All scaling. Ohmic ignition curves for f_L=4, 3.415, 3.2, 3.1. Murakami and beta limits.

FIG. 5. NET, α_n=0.5, Kaye Big scaling. Ohmic ignition curves for f_L=3.5, 3.022, 2.8, 2.7. Murakami and beta limits.

FIG. 6. NET, α_n=0.5, Shimomura-Odajima scaling. Ohmic ignition curves for f_L=2.5, 1.927, 1.4, 1. Murakami and beta limits.

FIG. 7. NET, α_n=0.5, Rebut-Lallia scaling. Ohmic ignition curves for f_L=1.6, 1.4, 1.2, 1. Murakami and beta limits.

FIG. 8. NET, α_n=0.5, Kaye-Goldston scaling. Ohmic ignition curves for f_L=2.2, 1.765, 1.7, 1.6. Murakami and beta limits.

FIG. 9. NET, α_n=2, Goldston scaling. Ohmic ignition curves for f_L=1.9, 1.75, 1.686, 1.6815. Murakami and beta limits.

FIG. 10. NET, α_n=2, Kaye All scaling. Ohmic ignition curves for f_L=3, 2.655, 2.5, 2.4. Murakami and beta limits.

FIG. 11. NET, α_n=2, Kaye Big scaling. Ohmic ignition curves for f_L=3, 2.350, 2.2, 2.1. Murakami and beta limits.

FIG. 12. NET, α_n=2, Shimomura-Odajima scaling. Ohmic ignition curves for f_L=2, 1.4, 1.326, 1. Murakami and beta limits.

FIG. 13. NET, α_n=2, Rebut-Lallia scaling. Ohmic ignition curves for f_L=1.6, 1.4, 1.2, 1. Murakami and beta limits.

FIG. 14. NET, α_n=2, Kaye-Goldston scaling. Ohmic ignition curves for f_L=1.5, 1.375, 1.3, 1.24. Murakami and beta limits.

FIG. 15. Critical L-mode enhancement factor for ignition in NET as a function of the density peaking parameter α_n for the different energy confinement time scalings.

INTERNAL DISTRIBUTION

J.M. Ané, R. Aymar, I. Fidone, L. Laurent, C. Leloup, E.K. Maschke, P. Prévot, J. Tachon, G. Tonon.

PERSONAL EXTERNAL DISTRIBUTION

- J.D. Callen, Department of Nuclear Engineering, University of Wisconsin, Madison, WISCONSIN 53706-1687.

- F. Engelmann, The NET Team, Max-Planck-Institut für Plasmaphysik, Boltzmannstrasse 2, D-8046 Garching bei Munchen, RFA.

- C. Gourdon, IRF/DIR, Orme des Merisiers, CEN SACLAY.

- J. Horowitz, IRF/DIR, c/o Mme Chériot, Orme des Merisiers, CEN SACLAY.

- S.M. Kaye, Experimental Scientific Division, Princeton Plasma Physics Laboratory, P.O. Box 451, Princeton, NEW JERSEY 08544, USA.

- P. Lallia, RF Physics Group, JET Joint Undertaking, Abingdon, Oxon OX14 3EA, G.B.

- F.W. Perkins, Applied Physics Division, Princeton Plasma Physics Laboratory, P.O. Box 451, Princeton, NEW JERSEY 08544, USA.

- D.E. Post, Princeton Plasma Physics Laboratory, P.O. Box 451, Princeton, NEW JERSEY 08544, USA.

- P.H. Rebut, JET Joint Undertaking, Abingdon, Oxon OX14 3EA, G.B.

- A. Rogister, Institute of Plasma Physics, Kernforschungsanlage, Julich GmbH, Association EURATOM/KFA, Postfach 1913, D-5170 Julich 1, RFA.

- N.A. Uckan, Confinement Prospects Section, Oak Ridge National Laboratory, P.O. Box Y, Oak Ridge, TENNESSEE 37831, USA.

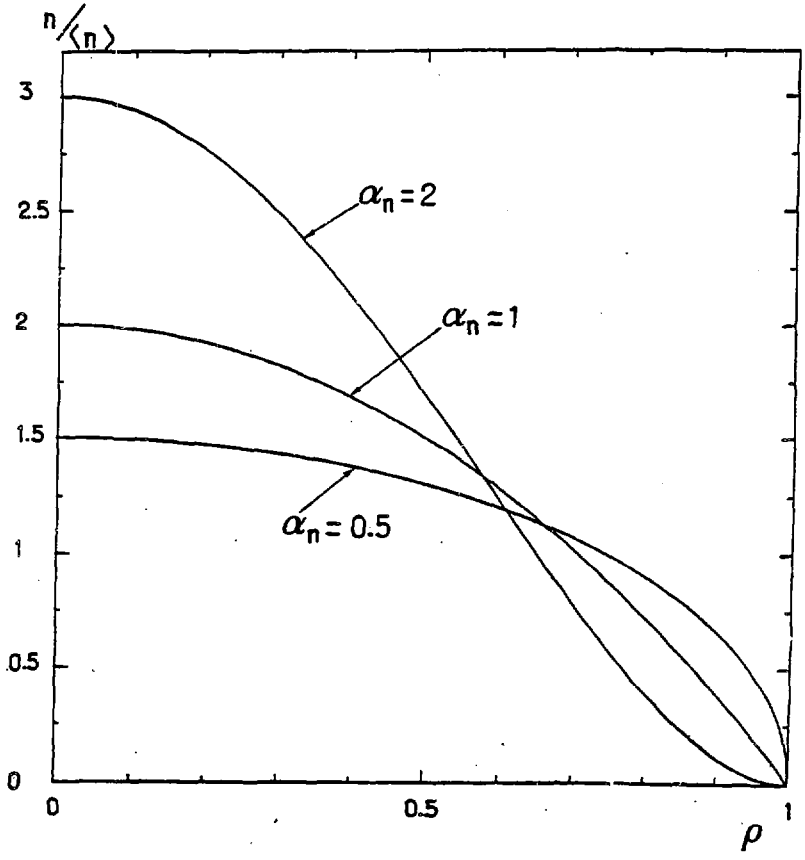

Fig. 1

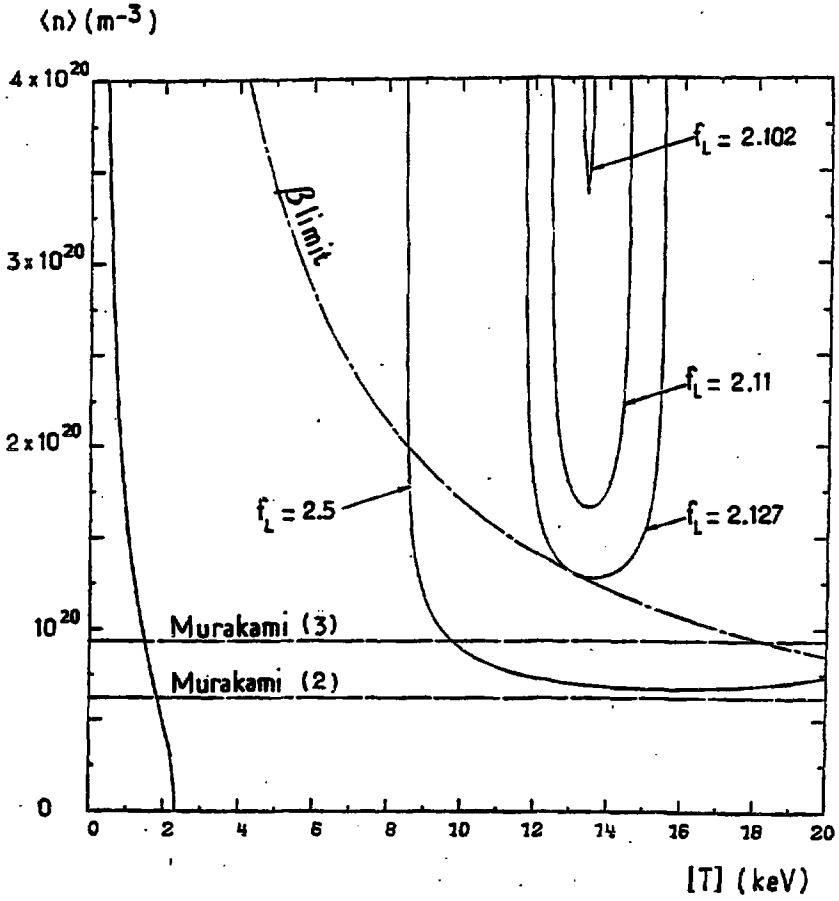
⟨n⟩ (m⁻³)
4 x 10²⁰
3 x 10²⁰
2 x 10²⁰
10²⁰
0
β limit
f_L = 2.102
f_L = 2.11
f_L = 2.127
f_L = 2.5
Murakami (3)
Murakami (2)
0
2
4
6
8
10
12
14
16
18
20
[T] (keV)

Fig. 2

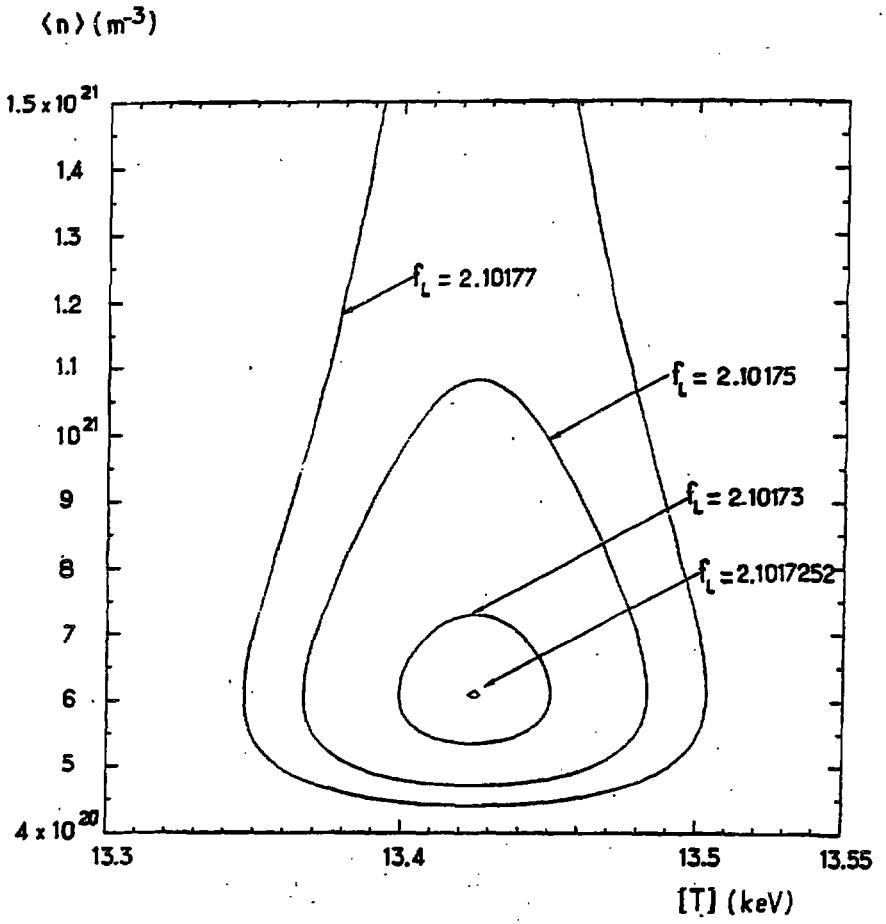
⟨n⟩ (m⁻³)
1.5 x 10²¹
1.4
1.3
1.2
1.1
10²¹
9
8
7
6
5
4 x 10²⁰
f_L = 2.10177
f_L = 2.10175
f_L = 2.10173
f_L = 2.1017252
13.3
13.4
13.5
13.55
[T] (keV)

Fig. 3

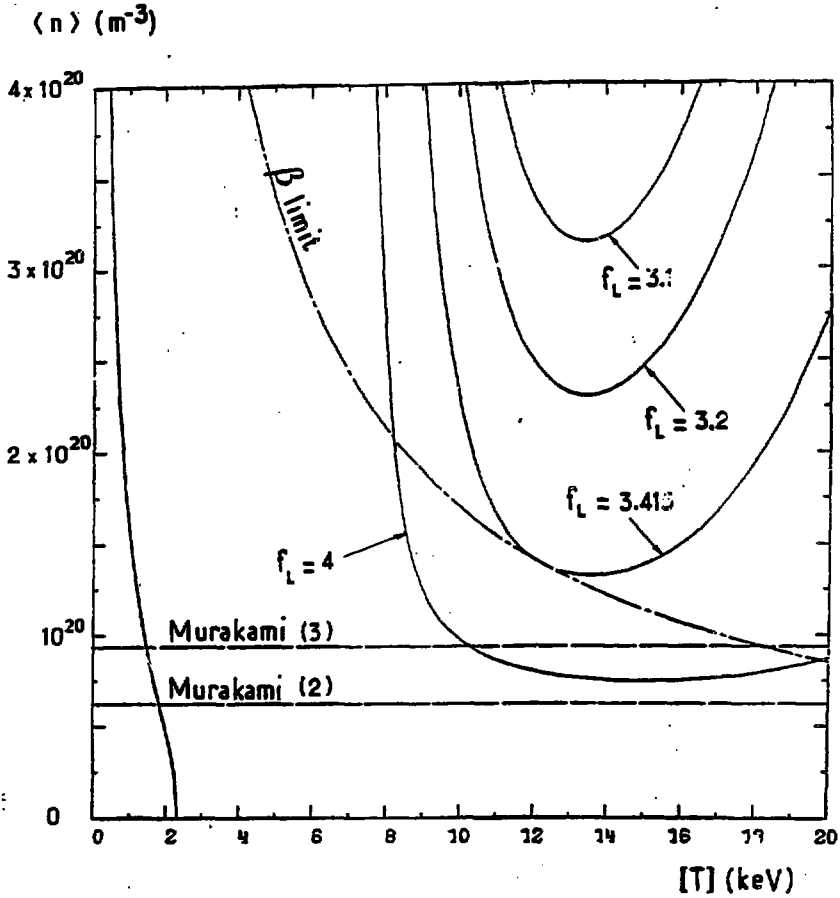
⟨n⟩ (m⁻³)
4x10²⁰
3x10²⁰
2x10²⁰
10²⁰
0
β limit
f_L = 3.1
f_L = 3.2
f_L = 3.415
f_L = 4
Murakami (3)
Murakami (2)
0
2
4
6
8
10
12
14
16
18
20
[T] (keV)

Fig. 4

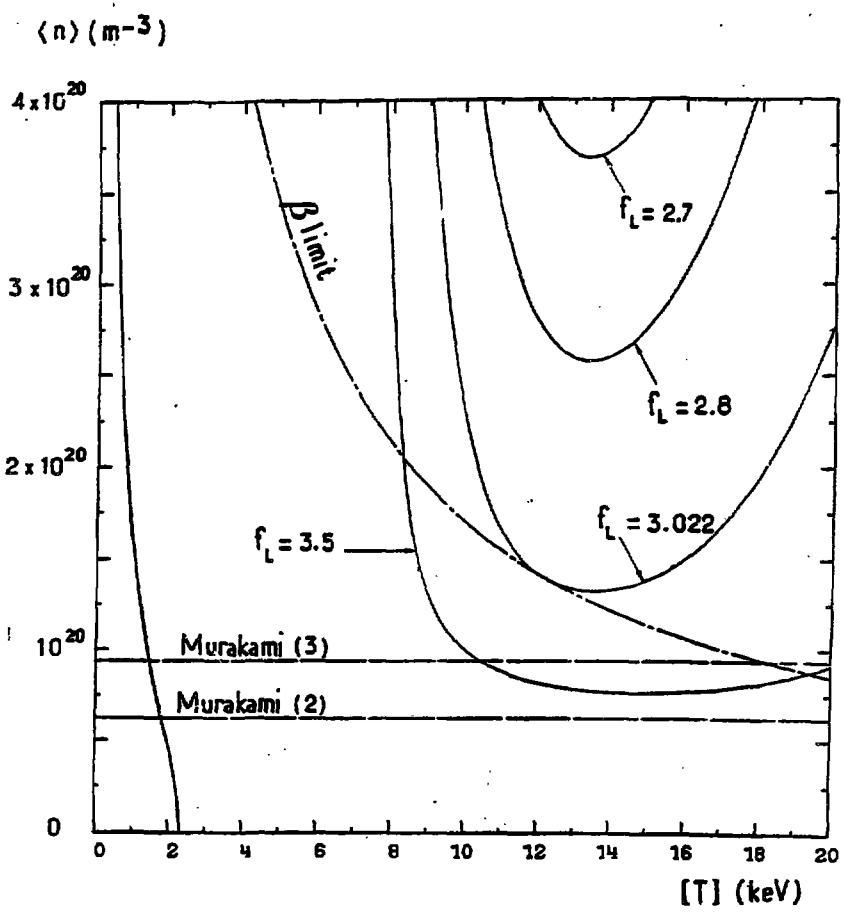
⟨n⟩ (m⁻³)
4x10²⁰
3 x 10²⁰
2 x 10²⁰
10²⁰
0
β limit
f_L = 2.7
f_L = 2.8
f_L = 3.022
f_L = 3.5
Murakami (3)
Murakami (2)
0
2
4
6
8
10
12
14
16
18
20
[T] (keV)

Fig. 5

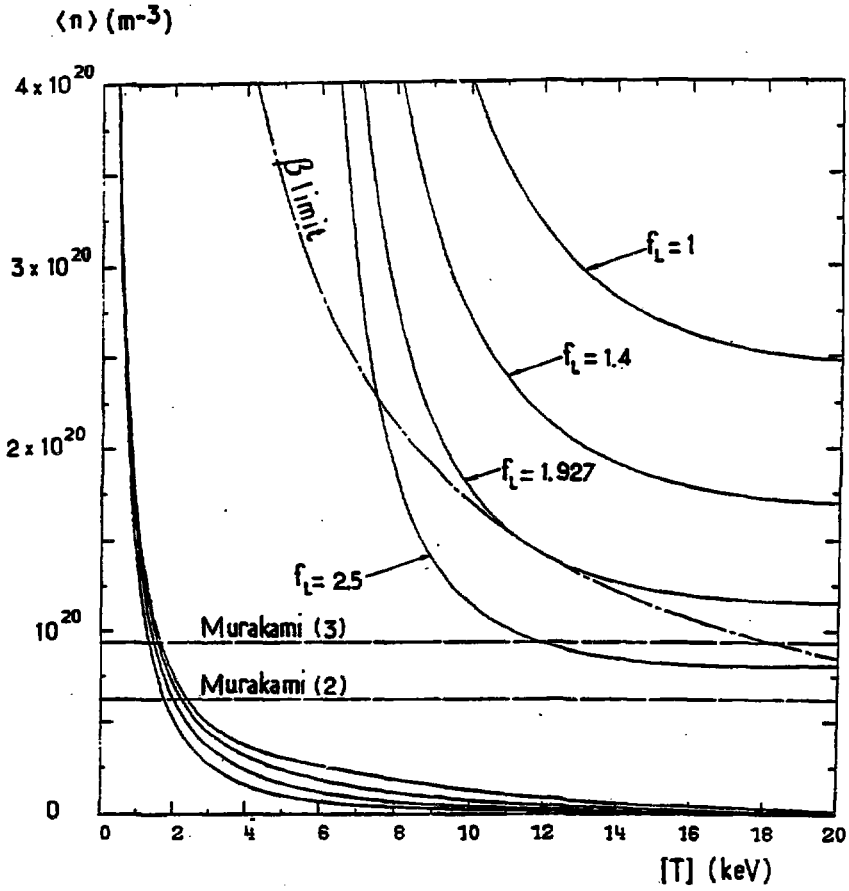
⟨n⟩ (m⁻³)
4 x 10²⁰
3 x 10²⁰
2 x 10²⁰
10²⁰
0
β limit
f_L = 1
f_L = 1.4
f_L = 1.927
f_L = 2.5
Murakami (3)
Murakami (2)
0
2
4
6
8
10
12
14
16
18
20
[T] (keV)

Fig. 6

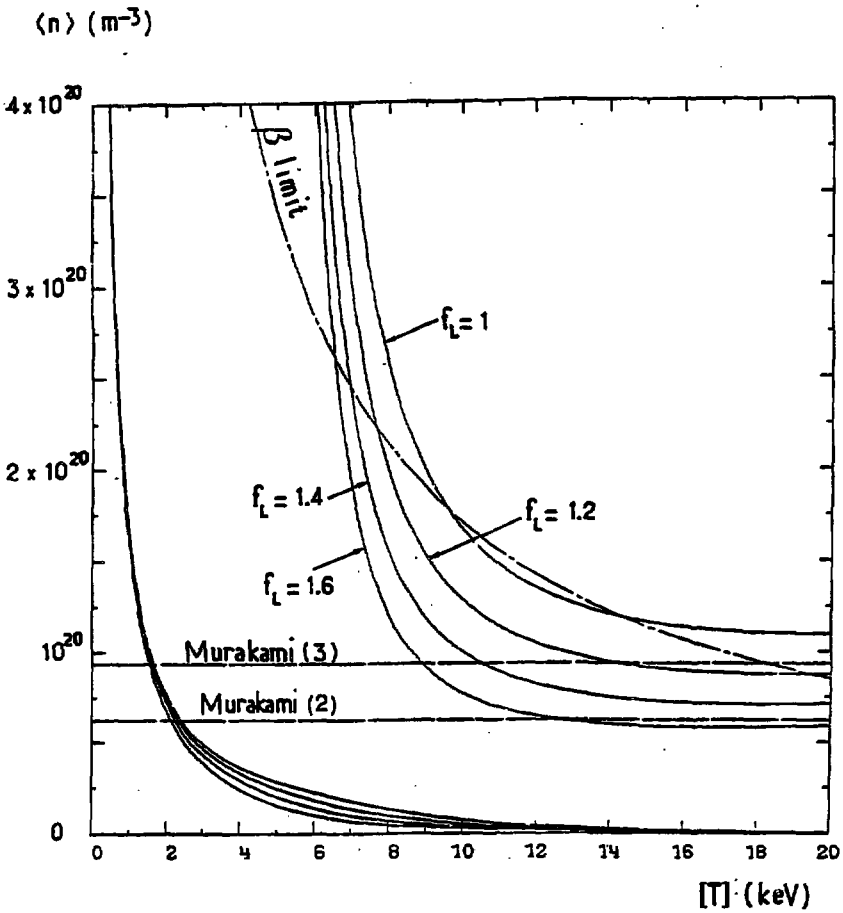
⟨n⟩ (m⁻³)
4 x 10²⁰
3 x 10²⁰
2 x 10²⁰
10²⁰
0
β limit
f_L = 1
f_L = 1.4
f_L = 1.2
f_L = 1.6
Murakami (3)
Murakami (2)
0
2
4
6
8
10
12
14
16
18
20
[T] (keV)

Fig. 7

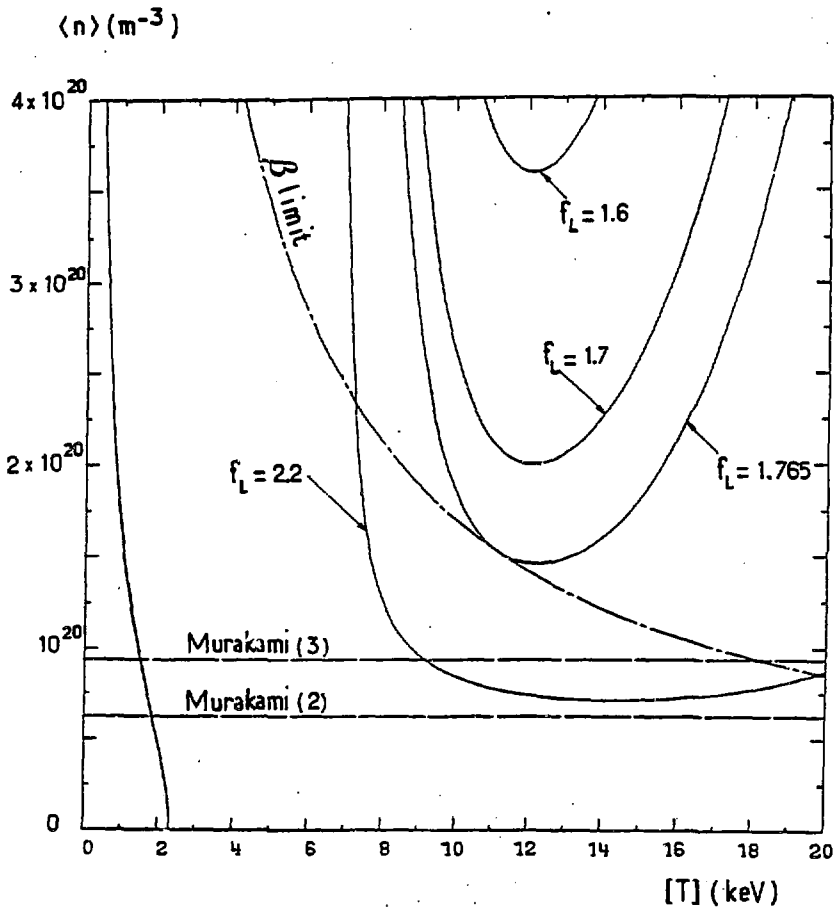
⟨n⟩ (m⁻³)
4 x 10²⁰
3 x 10²⁰
2 x 10²⁰
10²⁰
0
β limit
f_L = 1.6
f_L = 1.7
f_L = 2.2
f_L = 1.765
Murakami (3)
Murakami (2)
0
2
4
6
8
10
12
14
16
18
20
[T] (keV)

Fig. 8

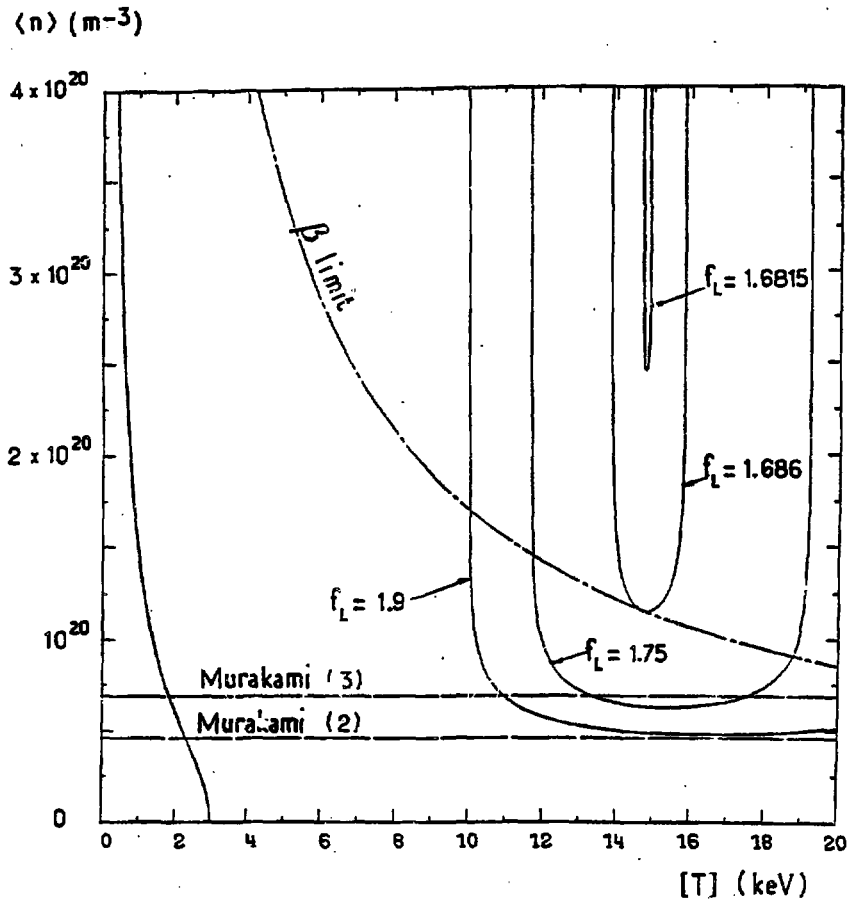
⟨n⟩ (m⁻³)
4 x 10²⁰
3 x 10²⁰
2 x 10²⁰
10²⁰
0
β limit
f_L = 1.6815
f_L = 1.686
f_L = 1.9
f_L = 1.75
Murakami (3)
Murakami (2)
0
2
4
6
8
10
12
14
16
18
20
[T] (keV)

Fig. 9

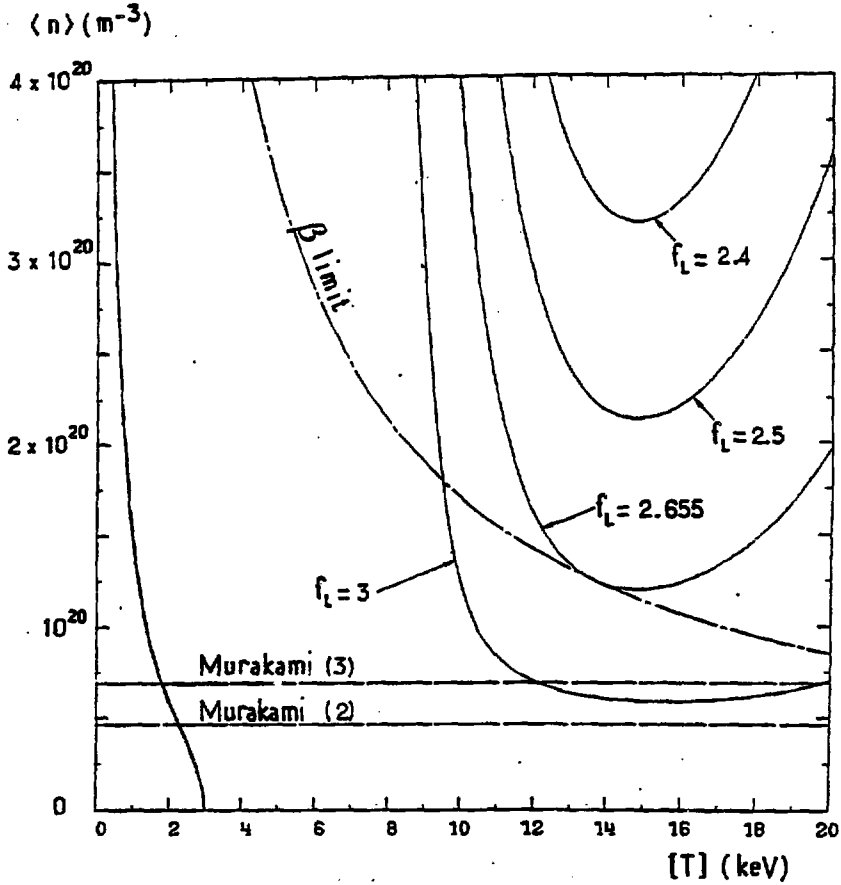
⟨n⟩ (m⁻³)
4 x 10²⁰
3 x 10²⁰
2 x 10²⁰
10²⁰
0
β limit
f_L = 2.4
f_L = 2.5
f_L = 2.655
f_L = 3
Murakami (3)
Murakami (2)
0
2
4
6
8
10
12
14
16
18
20
[T] (keV)

Fig. 10

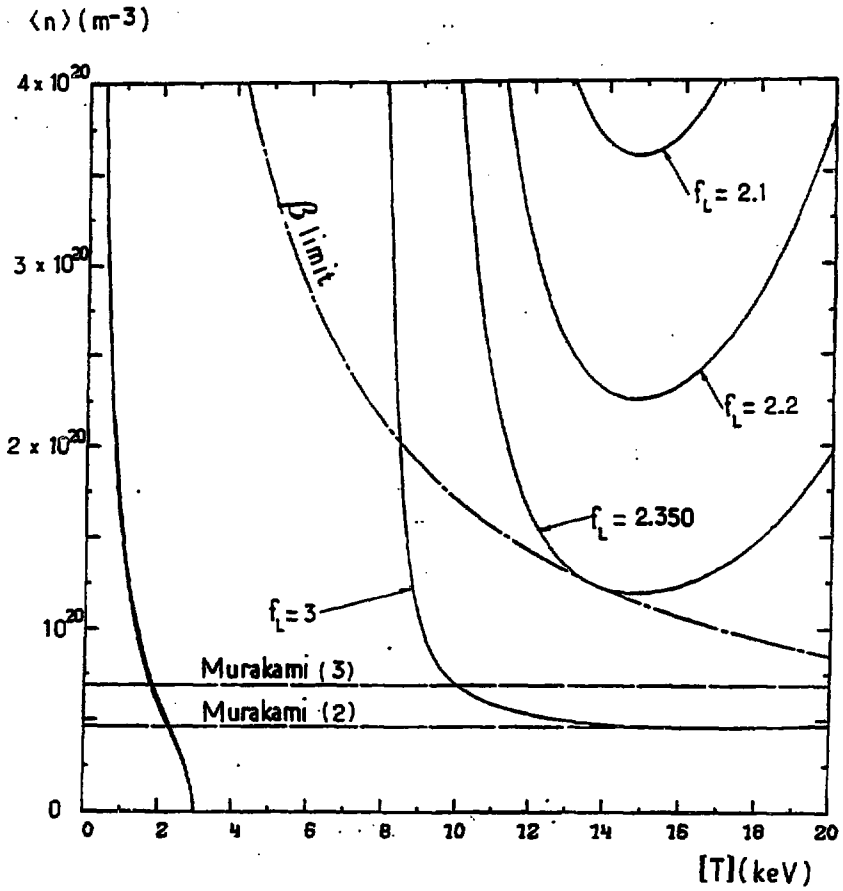
⟨n⟩(m⁻³)
4 x 10²⁰
3 x 10²⁰
2 x 10²⁰
10²⁰
0
β limit
f_L = 2.1
f_L = 2.2
f_L = 2.350
f_L = 3
Murakami (3)
Murakami (2)
0
2
4
6
8
10
12
14
16
18
20
[T](keV)

Fig. 11

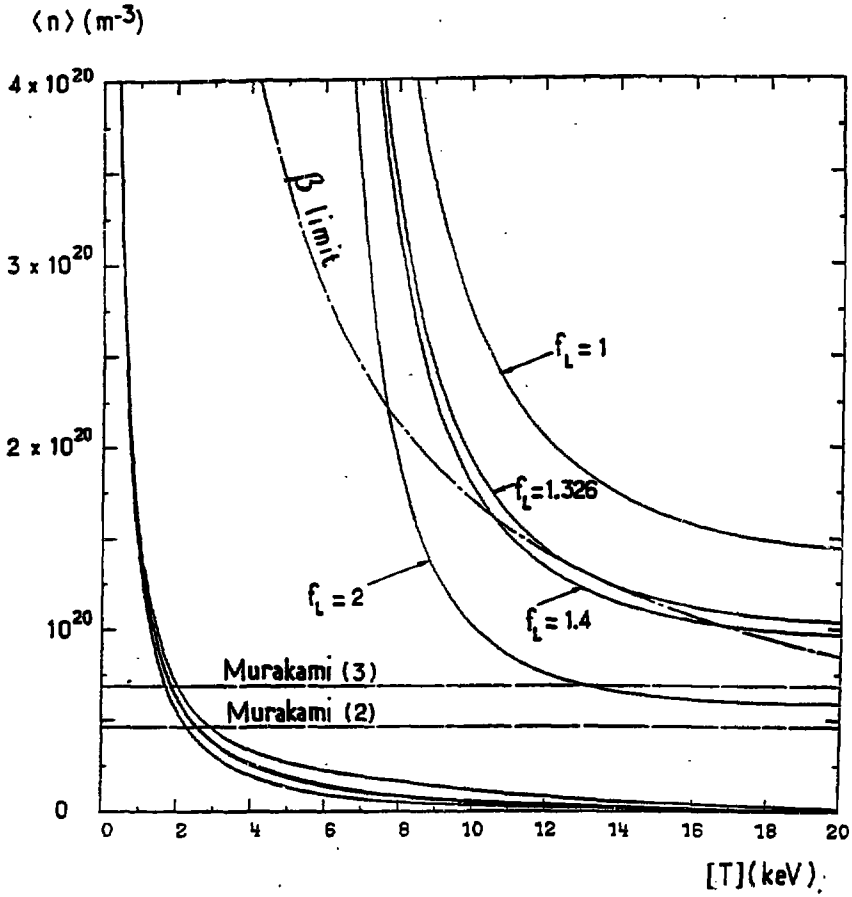
⟨n⟩ (m-3)
4 x 10^20
3 x 10^20
2 x 10^20
10^20
0
β limit
f_L = 1
f_L = 1.326
f_L = 2
f_L = 1.4
Murakami (3)
Murakami (2)
0
2
4
6
8
10
12
14
16
18
20
[T](keV)

Fig. 12

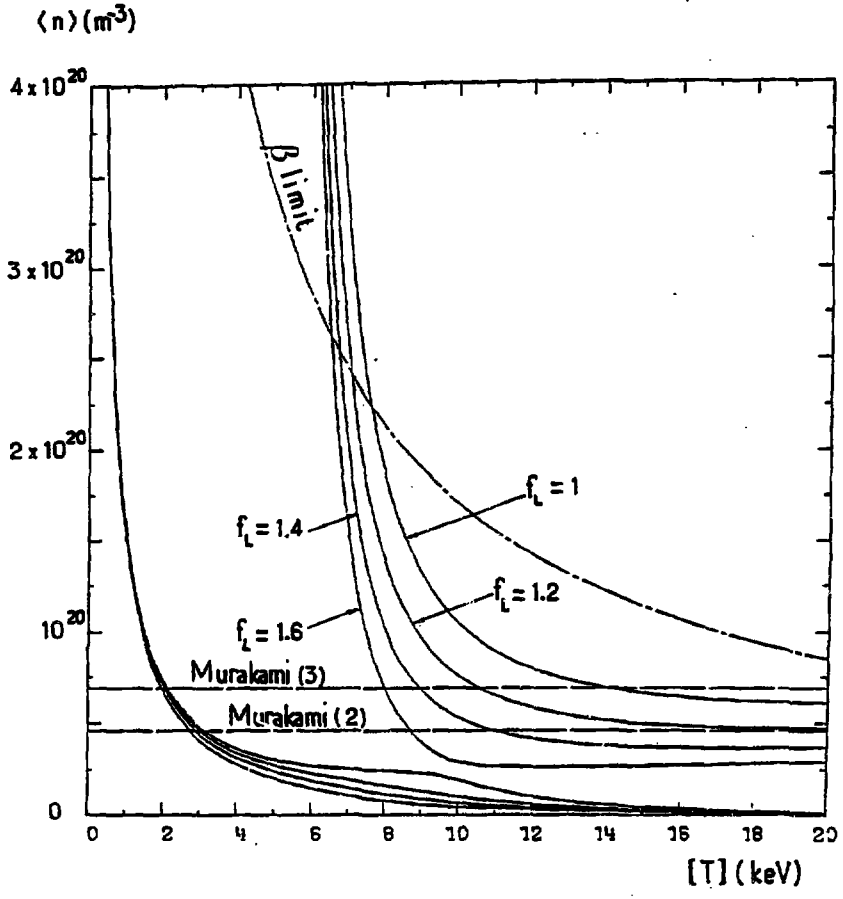
⟨n⟩(m³)
4x10²⁰
3x10²⁰
2x10²⁰
10²⁰
0
β limit
f_L = 1
f_L = 1.4
f_L = 1.2
f_L = 1.6
Murakami (3)
Murakami (2)
0
2
4
6
8
10
12
14
16
18
20
[T] (keV)

Fig. 13

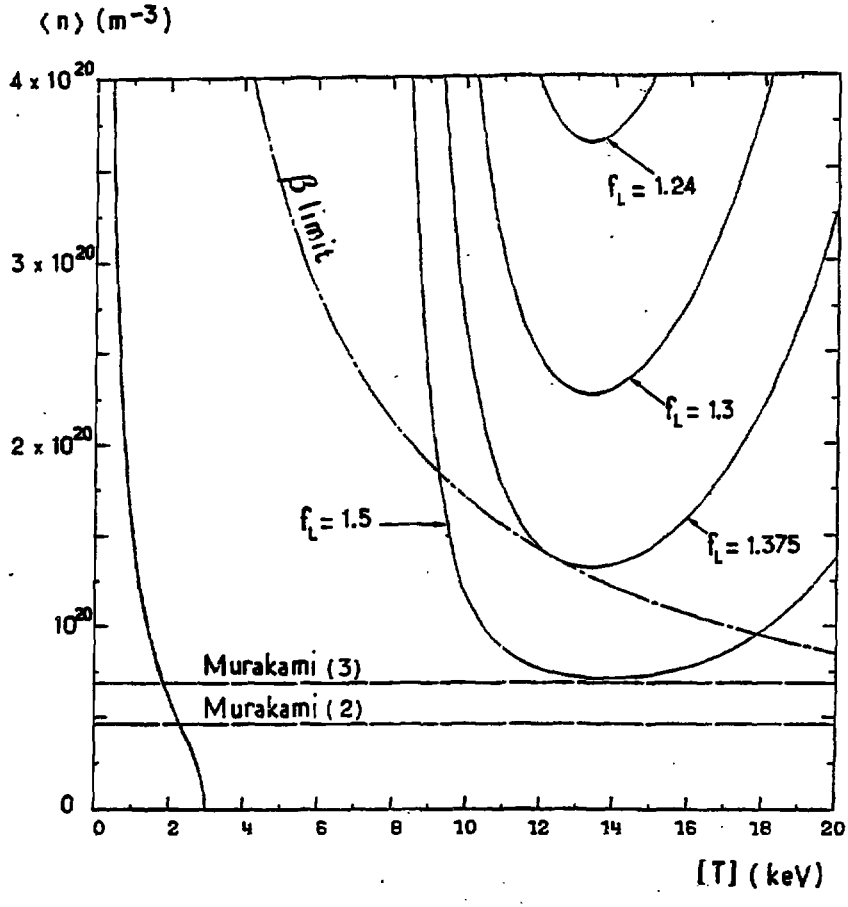
⟨n⟩ (m⁻³)
4 x 10²⁰
3 x 10²⁰
2 x 10²⁰
10²⁰
0
β limit
f_L = 1.24
f_L = 1.3
f_L = 1.5
f_L = 1.375
Murakami (3)
Murakami (2)
0
2
4
6
8
10
12
14
16
18
20
[T] (keV)

Fig. 14

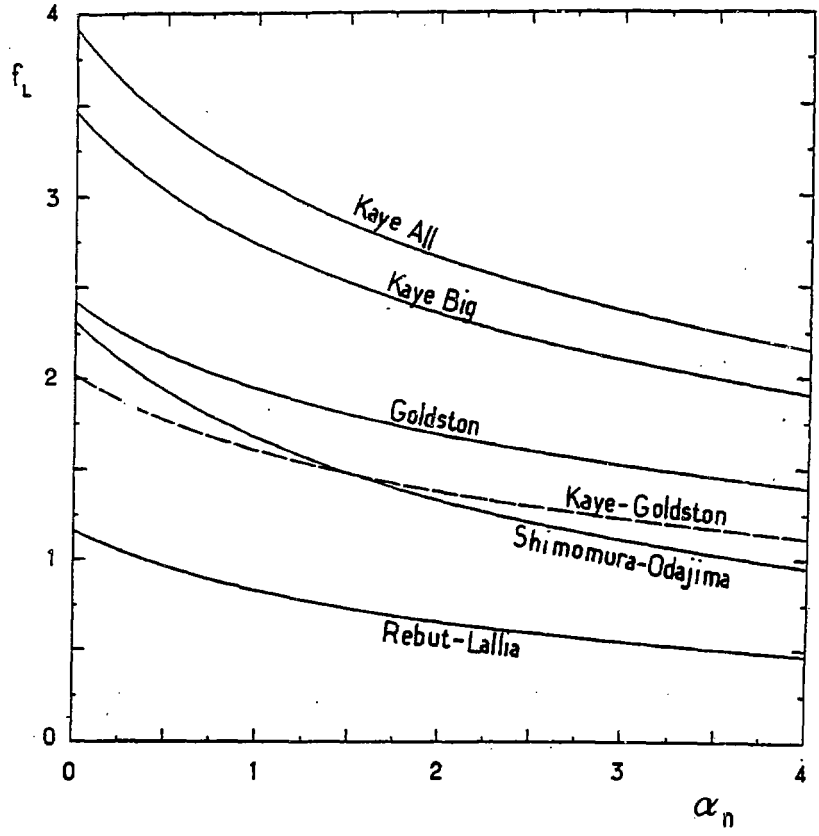
4
3
2
1
0
f_L
Kaye All
Kaye Big
Goldston
Kaye-Goldston
Shimomura-Odajima
Rebut-Lallia
0
1
2
3
4
α_n

Fig. 15